Evaluation of Local Strain Evolution from Metallic Whisker Formation

Yong Sun[1], Elizabeth N. Hoffman[2,*], Poh-Sang Lam[2], Xiaodong Li[1,*]

[1]Department of Mechanical Engineering, University of South Carolina, 300 Main Street, Columbia, SC 29202

[2]Savannah River National Laboratory, Aiken, SC 29808

* Corresponding authors, emails: elizabeth.hoffman@srnl.doe.gov; lixiao@cec.sc.edu

ABSTRACT

Evolution of local strain on electrodeposited tin films upon aging has been monitored by digital image correlation (DIC) for the first time. Maps of principal strains adjacent to whisker locations were constructed via comparing pre- and post-growth scanning electron microscopy (SEM) images. Results showed that the magnitude of the strain gradient plays an important role in whisker growth. DIC visualized the dynamic growth process in which the alteration of strain field has been identified to cause growth of subsequent whiskers.

Electronic device failure caused by spontaneous whisker growth from solder and plating materials has been known for over a half century [1]. Such phenomenon can be highly detrimental in microelectronic circuits where devices are separated by spacings as small as tens of nanometers. Historically lead (Pb) has been added to the solders to prevent whisker growth. Due to the harmful effects on human health and environments, it is no

longer a valid solution to prevent whisker growth with lead. With the shift to whisker-prone “Pb-free” solders, controlling whisker growth from low melting point metals has again become technically challenging.

It is generally acknowledged that internal stresses arising in low melting point metals, such as Sn, In, Cd, Bi, and Zn, promote whisker growth through a creep-like process [2]. Continuous effort has been made to search for a mechanism for whisker growth and several theories [3-6] have been put forth. While uncertainty remains pertaining to the stress source or sources responsible for whisker growth, it is generally agreed that 1) whiskers grow from the root [7]; 2) whisker growth is a result of a stress relaxation mechanism resulting from the underlying compressive stress [4, 8]; and 3) a thin film of low melting point metal is required for whisker growth [9]. The introduction of reliable lead-free solders into microelectronics manufacturing requires deeper understanding of this failure mechanism, which is complicated by several potential driving forces in the multi-material system.

In order to fully comprehend the driving force(s) of whisker growth, several analytic methods, i.e. X-ray diffraction (XRD) [10] and synchrotron [4, 11], as well as numerical method, i.e. finite element method (FEM) [12], have been applied for measuring residual stress/strain in thin metallic films with whisker growth. However, each technique has its limitations, especially for the analytic methods. XRD is not able to measure localized strain/stress state while synchrotron is too delicate for multi-time observations throughout the growth process. Such situation raises a question: is there a more adequate way to

monitor the local, yet dynamic evolution of strain/stress during the growth of whiskers? In the current study, such evolvement prior to and following the whisker growth was measured and evaluated with the aid of digital image correlation (DIC), for the first time to our knowledge. DIC is a capable tool for mapping local displacement and strain fields through computation of full-field displacements, strains, and strain rates on a sample surface [13-14]. DIC offers a convenient way to simultaneously achieve both full field visualization and dynamic evaluation of the stress/strain state at the local level, which can give an insight into the mystery and uncertainty of whisker growth.

Sn and SnPb thin films on Cu substrates were fabricated by electrodeposition. Please refer to the supporting materials for the details of process. All the samples have a spherical grain feature, which was typical for electrodeposition. Traditionally, DIC has been employed in the field of micro- and macro-scale deformation measurement with optical microscope images. Due to diffraction limitation of optical images, such analysis has a spatial resolution limit greater than 1 μm. Recently, DIC has been extended to sub-micron range along with high-magnification surface measurement tools such as scanning electron microscopy (SEM) and atomic force microscopy (AFM) [15-17]. In the current study, DIC technique was integrated with SEM to monitor the local in-plane strain evolvement on the sample surface before and after whisker growth. The SEM offers digital data storage, ability to post-process data with a range of desirable spatial resolutions, and excellent depth of field. These provide a necessary condition for equipment integration with the currently available DIC platforms to measure small

displacements down to the scale of microns on the grains around the growing whiskers, which have a representative diameter of 2-5 μm in the current study.

The distinct spherical characteristics of thin film morphology can be used in place of an artificially applied speckle pattern without further modification on the sample surface. This unique feature is especially advantageous for the current application with DIC, since the artificial patterns or gratings will obscure the observation of local whisker activities. A series of images on identical locations of the samples were taken with SEM (Quanta 200, FEI) using a constant voltage of 30 kV and a constant spot size of 5 μm in consecutive sessions, before and after whiskers were visually present. Resolution of the images was held constant at 1024×968 pixels. During intervals between the contiguous SEM sessions, which were from a couple to ~20 days, the samples were kept at ambient environment (~23°C and ~30-60% relative humidity or RH without controlling the ambient atmosphere). An array of Vickers indentation marks was made at different locations. These depressed sites served as an additional source of compressive stress/strain in addition to the residual stress from film deposition, and as markers to identify the areas of observation during the SEM sessions. For the Sn thin film deposited on copper, hillocks/whiskers were visually identified a few days after deposition. In contrast, no observable whisker growth was found on SnPb thin films after a considerable period of time.

The images of the areas of interest were analyzed using a Vic-2D DIC package (Correlated Solutions, Inc., Columbia, SC) software for an incremental correlation. The

images taken in the first session were used as reference images (initial state). All other images taken at later times from the same sample were compared to the reference image for constructing the two-dimensional surface in-plane displacement field, from which the strain distribution on the film surface could be calculated. It is well accepted that whisker growth is a diffusion phenomenon driven by residual compressive stress [8]. In the case of a thin film, localized stress state can be easily related to the strain field on the surface, which makes DIC an effective tool for visualizing the progression of stress generation and relaxation, before and after the whisker growth. Since Sn on copper finish had the highest whisker growth rate, majority of the DIC analysis were carried out on pure Sn thin films. Another reason to focus on the pure Sn thin films is that these samples had a relatively flat surface. Since only two-dimensional strain state could be evaluated by the present DIC package, it was necessary to minimize the out-of-plane strains by observing the flat areas if possible.

When the whisker forms on the sample surface, its elongation in length causes large in- and out-of-plane displacements, which can serve as sources of displacement discontinuity similar to cracks in fracture. One of the technical challenges for monitoring the strain evolution is to overcome the error due to poor correlation from DIC near and at the root of a whisker. This issue can be avoided in some cases when the initial or early stage of the whisker growth is captured by SEM observation before the whisker significantly alters the local morphology. Figure 1 shows an area that was observed by SEM shortly after the deposition was complete, and 1, 15, and 20 days after deposition, respectively. It is observed that a whisker has started growing after about 15 to 20 days (denoted by a

circle and pointed by an arrow in Figure 1d). The length of the whisker is relatively short comparing to the other whiskers found outside of this AOI, leading to a nearly non-obstruct view of the adjacent morphology, which is a necessary condition for a valid DIC evaluation. The strain field around the whisker location was calculated from the displacement field. Instead of giving the strain components with respect to each image orientation ($\varepsilon_{xx}/\varepsilon_{yy}/\varepsilon_{xy}$), the principal strains ($\varepsilon_1/\varepsilon_2$) are presented since the elongation and compression of local grains are of the most interest in the case of whisker growth. The area of interest (AOI) was a rectangular region of ~55×45 μm (162×132 pixels), with a subset size (L) of 35×35 pixels and a step size (δ) of 3 pixels. All the parameters were deliberately chosen for optimizing the image correlation coefficient.

Images taken one day after deposition were compared to the as-deposited ones, showing excellent correlation quality and $\varepsilon_1/\varepsilon_2$ are well below ±0.1%. Such results demonstrate the accuracy of the methodology and validate further correlation processes. The strain detected during the period of observation falls into a range of ±0.6%, indicating that the Sn grains near whisker growth locations yield plasticity. Such result is consistent with reported stress measurements [5, 12]. From Figure 1c, moderate compressive strain was usually detected a couple of grains apart from the growth location, which is denoted by the black open circle by comparing to Figure 1d. Figure 1c clearly indicates that considerable compressive strain and strain gradient are present around the root of spontaneously growing Sn whisker during the incubation period (see the red open circles on the figure). Note that there is a weak tensile strain near the specific location. This is consistent with the observations that stress gradient [18] or residual strain-gradient [11]

can be responsible for the whisker growth instead of a sole compressive field. The current results imply that the strain or stress gradient would be a driving force for whisker growth, assuming that these gradients provide a path for fast diffusion. It is also intriguing to notice the evolution of strain during the initial growth of the whiskers. The strain contours in Figure 1d show a significant change from those in Figure 1c. It should be noted that the noticeable tensile strain on the location of whisker growth for ε_1 can be over-evaluated due to the displacement aroused by the elongation of the whisker. Nevertheless, distinct compressive strains were also present in a few locations, especially for ε_2.

A few theories, for example, grain boundary diffusion [12, 19], grain boundary fluid theory [8] and interface fluid flow [20], have been suggested as possible mechanisms for tin whisker growth, each of which have been supported by experimental observations in different cases. The considerable compressive strain here can be caused by shrinkage of the grains, indicating that grain boundary related activity is the main factor in such growth process. Comparing to Figure 1c (15 days), the strain gradient around the whisker shown in Figure 1d (20 days) is much higher, without any sign of relaxation of local strain due to whisker growth. This intensified strain gradient may serve as a sustainable driving force for whisker growth. Such hypothesis is supported by the observation that a second whisker sprouted out next to the existing whisker in about 40 days. However, the excessive morphology change did not allow a valid DIC measurement and therefore, the strain distribution is not presented in this paper. (Please refer to the supporting materials for the appearance of the second whisker and the unsuccessful DIC calculation results.)

Conveniently, with mild modification, DIC can also capture the shift of local strain state during the consecutive growth of whiskers. Furthermore, it provides a facile route to explore the inter-relationship between adjacent whiskers and thus to evaluate and visualize the uncertainties in consecutive growth processes. Figure 2 illustrates the sequence of a consecutive growth of three whiskers observed at a different AOI on the same Sn film as in Figure 1. For analyzing the strain state after whisker growth, rectangular areas covering the whiskers were cropped out from the SEM images (Figs. 2b-e). Such measure was necessary because the current DIC methodology is unable to accurately correlate images with obstructed objects (in this case, the elongated whiskers) as mentioned earlier. (Please refer to the supporting materials for DIC without cropping). The size of the cropped area was determined by the size of the subset which is used for analysis with Vic-2D. In the present case, an AOI of 100×100 μm (~300×300 pixels) was selected, with a subset size of 39×39 pixels and a step size of 2 pixels. Multiple whiskers have been observed to grow successively out of the Sn surface during a period of 120 days. The images were taken after 35, 60, 75 and 120 days, respectively. Only mild principal strains were present around the first whisker. A generally compressive strain field can be seen in both principal directions around the second whisker prior to its growth. Figures 2c-d show a wavy band-like trend of tensile strain for ε_1. Such trend can be postulated as a sign of fast diffusion of Sn atoms between adjacent locations caused by the growing whiskers. At the same time, noticeable increase in compressive strain, especially ε_2, can be seen near the root of the third whisker, which is denoted by circles in Figure 2d. Such trend eventually triggers the growth of the third whisker.

The growth process is depicted graphically in Figure 3a, where the first whisker grows on a location with considerable compressive strain and large strain gradient. As the whisker continues to grow, the Sn atoms from adjacent areas diffuses continuously to the root of the first whisker, resulting in the relaxation of local compressive strain and the increase of tensile strain, as well as the strain gradient. While the first whisker ceases to grow, the second whisker would be triggered if the strain gradient reaches a critical value. Such a dynamic pattern will lead to consecutive whisker growth in certain areas on the Sn film. Line profiles extracted from the DIC results appear to support this hypothesis as shown in Figures 3b-3c, where $\varepsilon_1/\varepsilon_1$ from location A to location B (Fig. 2b) is plotted. It is clear that the strain near location A is greatly relaxed to almost neutral level, resulting in a decrease of whisker growth rate at location A. Meanwhile, a considerable strain gradient takes place near location B and is hypothetically responsible for the growth of the third whisker (see Fig. 2e) as a driving force for whisker growth. It should be noted that, although ε_1 near location B is still in tension after 75 days, it has been lowered to a level at which the compressive strain along the second principal direction (ε_2) dominates the whisker growth mechanism.

In summary, a methodology has been developed to incorporate DIC technique with SEM images for mapping the local strain fields during whisker growth. By processing SEM images taken in consecutive time intervals over the area of interest on Sn-Cu finishes, the local strain evolution due to whisker growth can be obtained. This methodology provides an alternative way for exploring the complicated process of whisker growth through the

morphology changes. From the DIC results, it is proposed that strain or stress gradient, instead of an overall compressive stress field is the key for whisker growth. Results from SEM and DIC analysis also indicate that the whisker growth is a continuously dynamic process, during which the subsequent whisker is triggered by the redistribution of strain or stress field after local strain relaxation. The findings have advanced the understanding of whisker growth mechanisms and may provide insight for developing whisker mitigation technology for lead-free solder alloys.

This work has been funded through DoD Strategic Environmental Research and Development Program (SERDP) under project WP-1754.

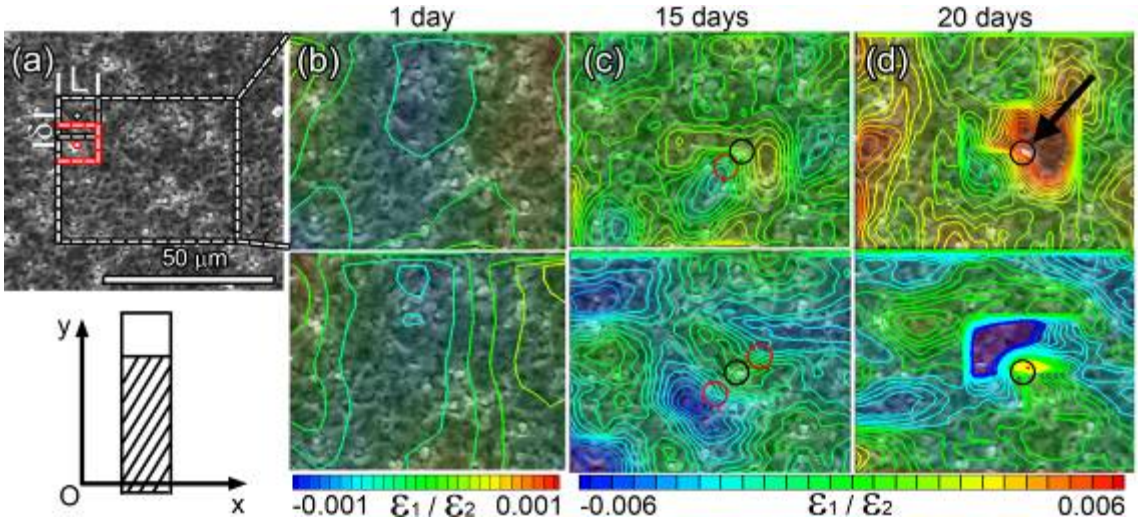

Figure 1. The reference image taken on a Sn film, immediately after electrodeposition (a) with the AOI and subset outlined by dotted line and DIC results of ε_1 (first row) and ε_2 (second row) based on images taken on identical locations after 1 day (b) 15 days (c) and 20 days (d) day after deposition. Black circles/arrow in (c) and (d) denote the location of the whisker growth. The global coordinate system indicates axial and transverse directions.

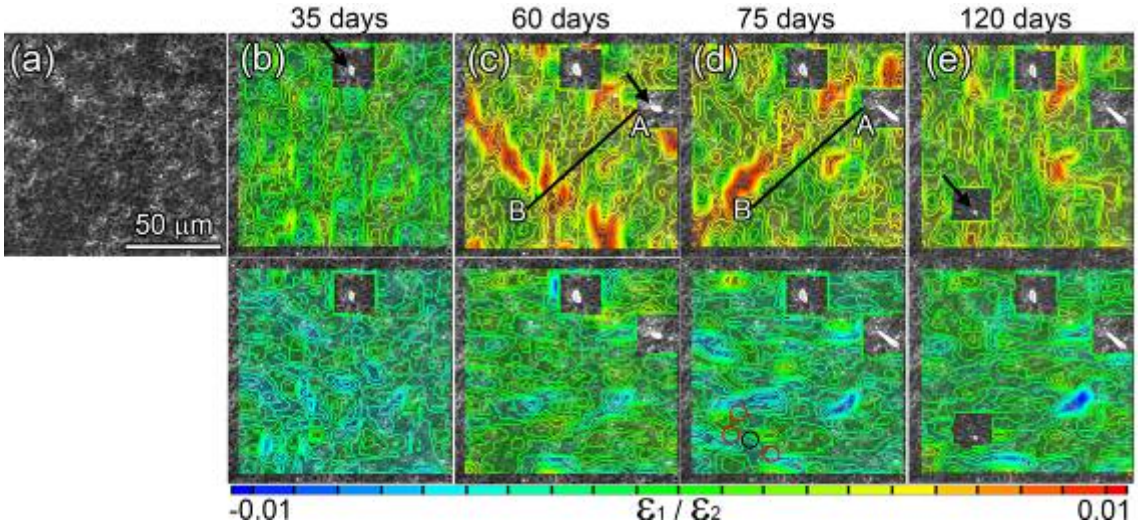

Figure 2. Another reference image taken on the Sn film, immdediately after electrodeposition (a) and DIC results of $\varepsilon_1/\varepsilon_2$ based on images taken on identical locations after 35 days (b), 60 days (c), 75 days (d) and 120 days (e).

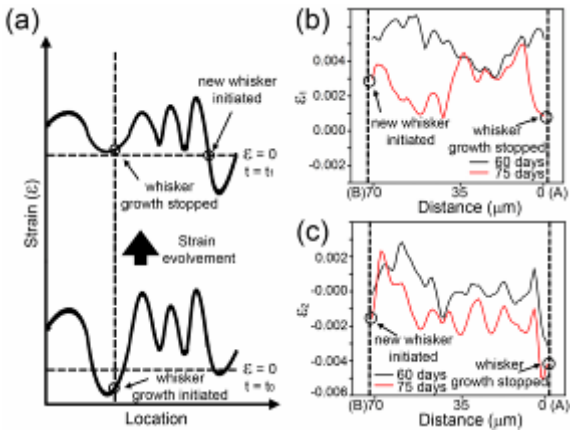

Figure 3. Sketch for dynamic evolution of local strain leading to consecutive whisker growth (a) and actual line profiles of ε_1 (b) and ε_2 (c) extracted from the strain contour (A to B in Figs. 3c-2d). Dotted lines in (b) and (c) indicate the location of the whiskers.

REFERENCES

[1] K.G. Compton, A. Mendizza, S.M. Arnold, Corrosion, 7 (1951) 365-372.
[2] W.J. Boettinger, C.E. Johnson, L.A. Bendersky, K.W. Moon, M.E. Williams, G.R. Stafford, Acta Materialia, 53 (2005) 5033-5050.
[3] K.N. Tu, Acta Metallurgica, 21 (1973) 347-354.
[4] W.J. Choi, T.Y. Lee, K.N. Tu, N. Tamura, R.S. Celestre, A.A. MacDowell, Y.Y. Bong, L. Nguyen, Acta Materialia, 51 (2003) 6253-6261.
[5] B.Z. Lee, D.N. Lee, Acta Materialia, 46 (1998) 3701-3714.
[6] M.W. Barsoum, E.N. Hoffman, R.D. Doherty, S. Gupta, A. Zavaliangos, Physical Review Letters, 93 (2004) 206104.
[7] S.E. Koonce, S.N. Arnold, Journal of Applied Physics, 24 (1952) 365-366.
[8] K.N. Tu, J.C.M. Li, Materials Science and Engineering: A, 409 (2005) 131-139.
[9] J.A. Nychka, Y. Li, F.Q. Yang, R. Chen, J. Electron. Mater., 37 (2008) 90-95.
[10] J.H. Zhao, P. Su, M. Ding, S. Chopiri, P.S. Ho, IEEE Transactions on Electronics Packaging Manufacturing, 29 (2006) 265-273.
[11] M. Sobiech, M. Wohlschlogel, U. Welzel, E.J. Mittemeijer, W. Hugel, A. Seekamp, W. Liu, G.E. Ice, Applied Physics Letters, 94 (2009) 221901.
[12] E. Buchovecky, N. Jadhav, A.F. Bower, E. Chason, J. Electron. Mater., 38 (2009) 2676-2684.
[13] M.A. Sutton, C. Mingqi, W.H. Peters, Y.J. Chao, S.R. McNeill, Image and Vision Computing, 4 (1986) 143-150.
[14] F. Hild, S. Roux, Strain, 42 (2006) 69-80.
[15] I. Chasiotis, W.G. Knauss, Experimental Mechanics, 42 (2002) 51-57.
[16] X.D. Li, W.J. Xu, M.A. Sutton, M. Mello, IEEE Transactions on Nanotechnology, 6 (2007) 4-12.
[17] Z.H. Xu, M.A. Sutton, X.D. Li, Acta Materialia, 56 (2008) 6304-6309.

[18] J. Liang, Z.H. Xu, X.D. Li, Journal of Materials Science: Materials in Electronics, 18 (2007) 599-604.
[19] K.N. Tu, Physical Review B, 49 (1994) 2030-2034.
[20] H.P. Howard, J. Cheng, P.T. Vianco, J.C.M. Li, Acta Materialia, 59 (2011) 1957-1963.

Supporting Information

Evaluation of Local Strain Evolution from Metallic Whisker Formation

Yong Sun[1], Elizabeth N. Hoffman[2], Poh-Sang Lam[2], Xiaodong Li[1]

[1]Department of Mechanical Engineering, University of South Carolina, 300 Main Street, Columbia, SC 29202

[2]Savannah River National Laboratory, Aiken, SC 29808

Electrodeposition of Sn and SnPb thin film on Cu substrates

Sn and SnPb thin films on Cu substrates were fabricated by electrodeposition in an electrochemical workstation (model 760D, CH Instruments, Austin, TX) with a three-electrode system. A titanium-mesh electrode with 10 μm thick platinum film was used as the counter electrode and the reference electrode was Ag/AgCl. Chemicals of analytical grade and double-distilled water were used throughout all experiments. For Sn deposition, sodium citrate tri-basic di-hydrate ($C_6H_5Na_3O_7 \cdot 2H_2O$) was added into a tin (II) chloride ($SnCl_2 \cdot 2H_2O$) aqueous solution to achieve a stable stannous solution [1]. A constant current density, 4 mA/cm^2, was applied to reach a homogenous and continuous thin film. Uniform coatings of SnPb (~50 wt% Sn and ~50 wt% Pb) were obtained with a methane-sulfonic acid (MSA) based bath with addition of tin (II) methanesulfonate ($(CH_3SO_3)_2Sn$) and lead nitrate ($Pb(NO_3)_2$) [2]. Chronopotentiometry deposition method with a cathodic current density of 20 mA/cm^2 was used during deposition. The morphology and compositional information of the coatings are displayed in Figures S1a-1b. The thickness of the samples was measured to be approximately 10 μm in the middle of the samples, as shown in Figure S1c. Such thin thickness is stated to be a precondition for observable

whisker growth [3]. The cross-section image also demonstrates a good bonding between the deposited films and the substrates.

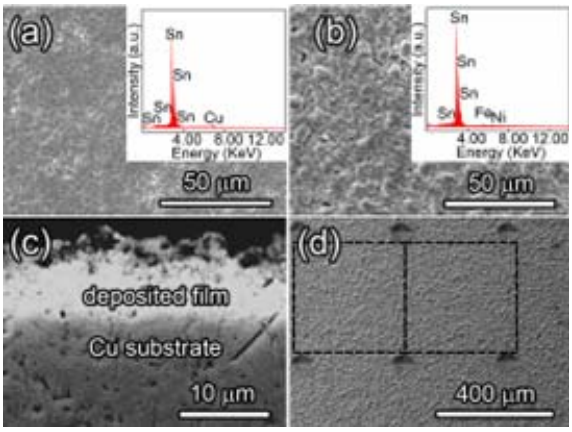

Figure S1. Surface morphology of Sn (a) and 50Sn50Pb (b) deposited on Cu, with compositional information from Energy-dispersive X-ray spectroscopy (EDX) shown in inlets; SEM images for cross section of a Sn-Cu finish (c); arrays of Vickers indentation marks (d) and the areas for imaging.

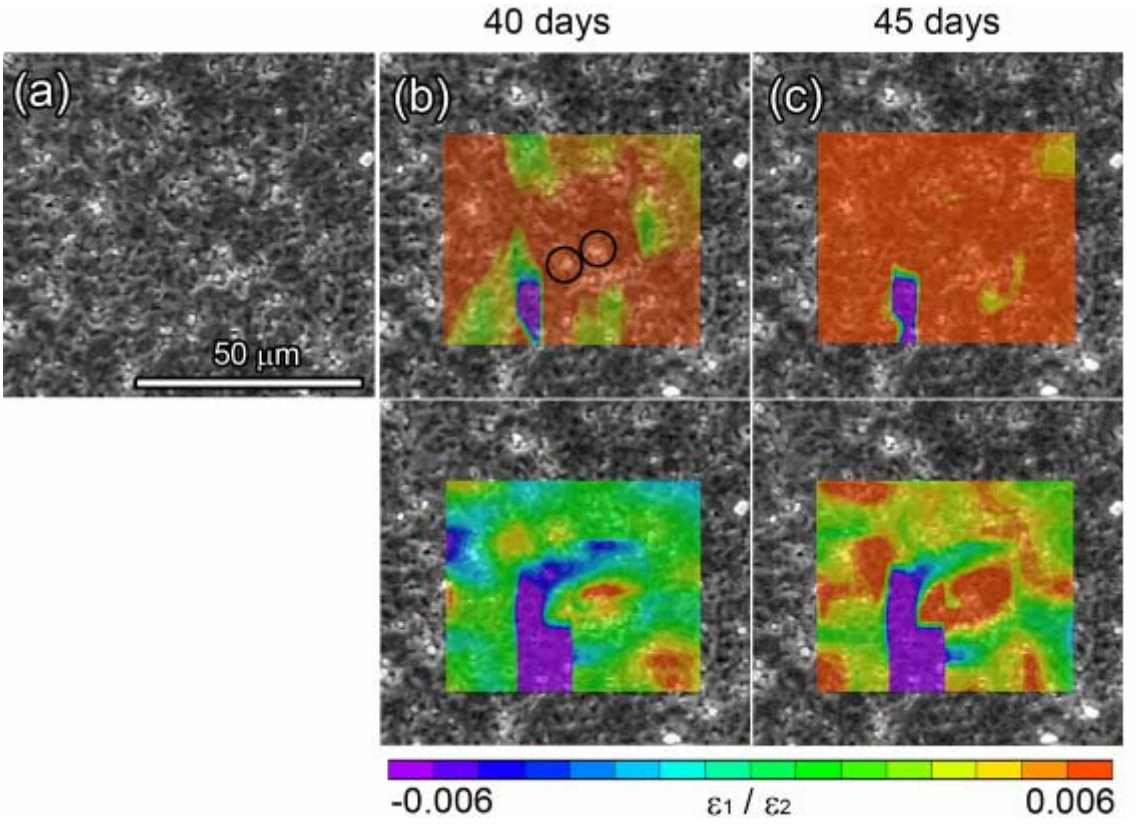

Figure S2. Reference image corresponding to Figure 2 (a) and images with full AOI DIC results of ε_1 (first row) and ε_2 (second row) based on images taken on identical locations after 40 days (b) and 45 days (c). Two neighboring whiskers are denoted in (b) by circles.

DIC results of Figure 1 after 20days

The second whisker sprouted out and was visually identified 45 days after the deposition. It changes the surface morphology drastically and thus leads to poor correlation of DIC. Figures S2(b)-(c) show such invalid results, indicating over-evaluated tensile strain on the location of the second whisker and extremely high compressive strains in adjacent areas.

Full AOI DIC results on identical location used in Figure 2

Same parameters, i.e. subset size of 39×39 pixels and step size of 2 pixels were used. Highly over-evaluated strains can be seen around the first whisker in Figure S3b.

Correlation is even worse in Fgures S3c-3e, around the areas where the second and the third whiskers grow. Especially for Figure 3e, the entire left part of the image is in poor correlation and extremely high compressive strains are present for both ε_1 and ε_2.

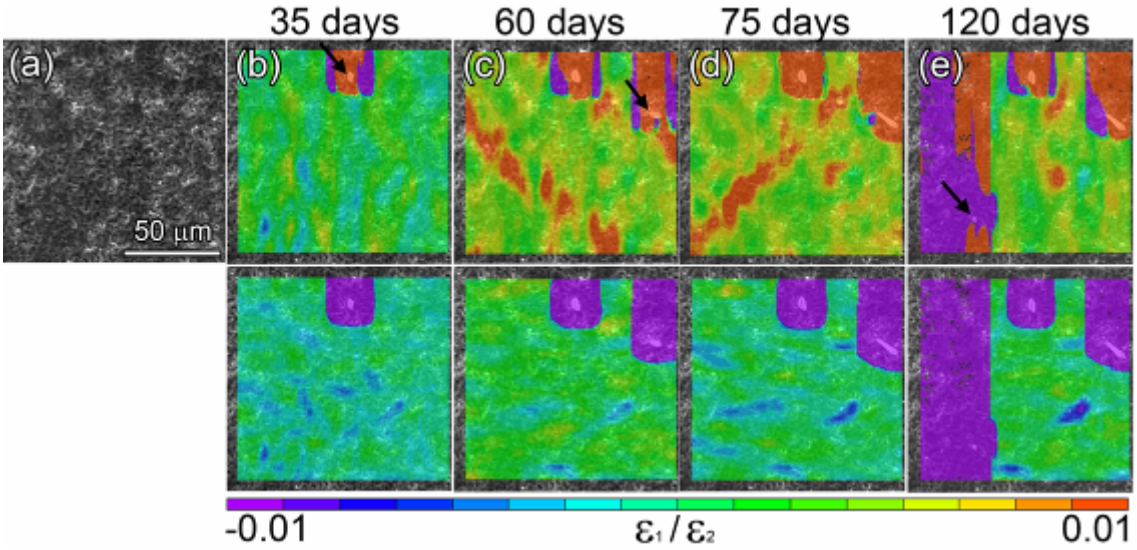

Figure S3. Reference image corresponding to Figure 3 (a) and images with full AOI DIC results of ε_1 (first row) and ε_2 (second row) based on images taken on identical locations after 35 days (b), 60 days (c), 75 days (d) and 120 days (e).

Reference

[1] A. He, Q. Liu, D. Ivey, Journal of Materials Science: Materials in Electronics, 19 (2008) 553-562.
[2] J.L.P. Siqueira, I.A. Carlos, Journal of Power Sources, 169 (2007) 361-368.
[3] F.Q. Yang, Y. Li, Journal of Applied Physics, 104 (2008) 113512.